



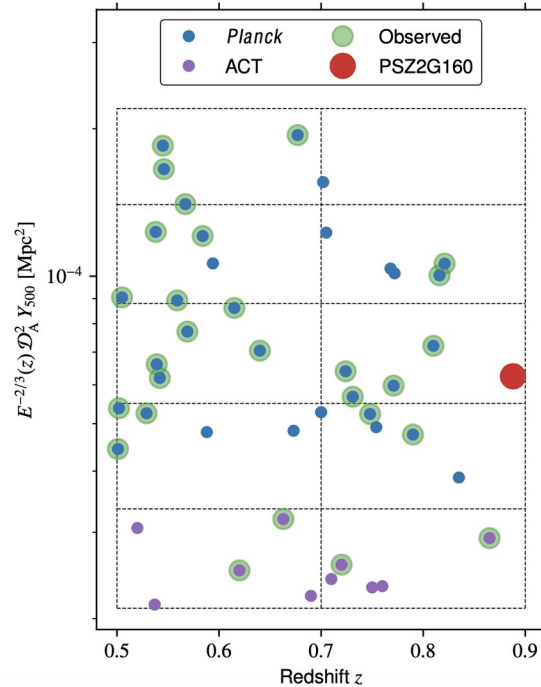
Multi-probe analysis of the galaxy cluster **CLJ1227:** unveiling **systematics in mass estimation**

Miren Muñoz Echeverría, LPSC, Grenoble
on behalf of the NIKA2 collaboration

mm Universe @ NIKA2 – 28.06.2021



NIKA2 Sunyaev-Zel'dovich Large Program

Study of 45 high redshift galaxy clusters



One of the **objectives**...

...**hydrostatic mass estimate** combining:

- Electron pressure from thermal SZ effect with 
- Electron density and temperature from X-rays with 

XMM-Newton

Which **systematic errors** can affect the hydrostatic mass estimate?

How is this mass **compared to other estimations**?

The cluster: CLJ1227 or PSZ2G160

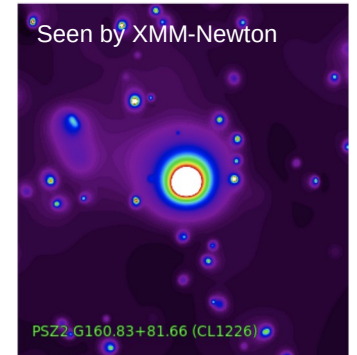
Prior knowledge of the cluster

(Planck SZ 2)

z	0.888
$Y_{500} [10^{-3} \text{arcmin}^2]$	0.38
$\theta_{500} [']$	1.9
$M_{500} [10^{14} M_{\odot}]$	5.7

← Highest redshift cluster of the NIKA2-LPSZ

- The **main clump**:
 - centered on the BCG (Zitrin et al., 2009)
 - BCG, X-ray peak and the galaxy number density peak seem to match (M.Jee and J.Tyson, 2009)
- The **secondary clump**:
 - A hot substructure / overdensity at $\sim 40''$ to the southwest of the center (B. J. Maughan et al., 2007, M.Jee and J.Tyson, 2009)
 - Correlated to the cluster galaxy distribution (M.Jee and J.Tyson, 2009)



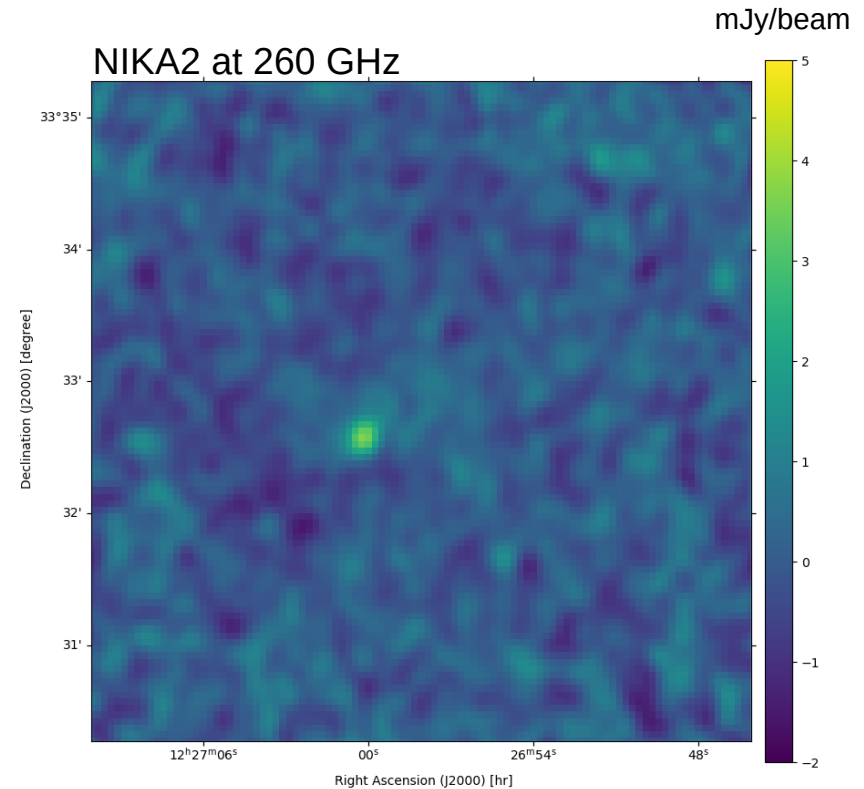
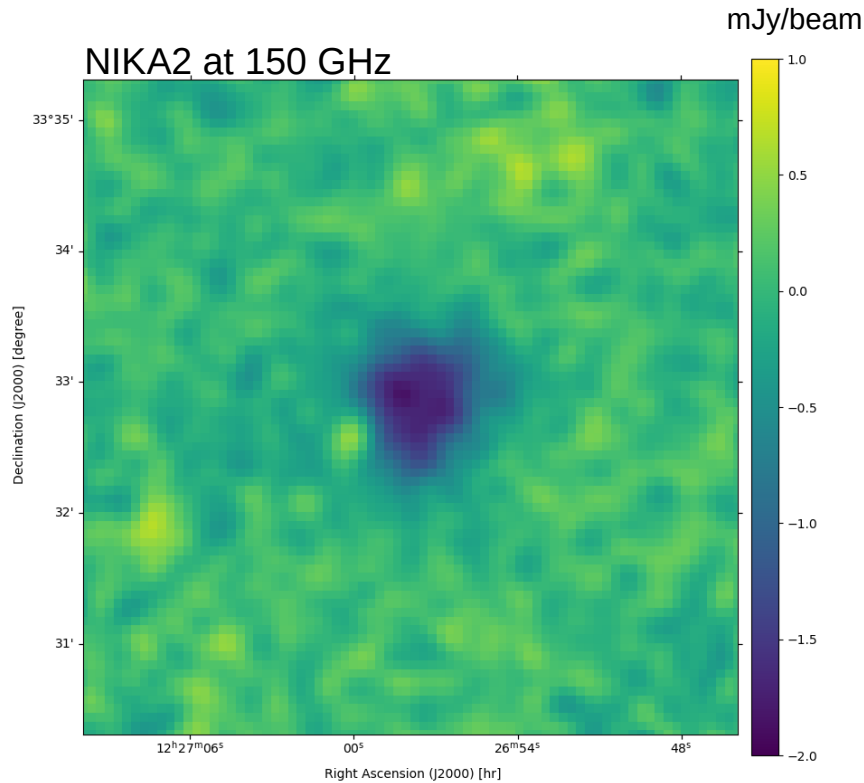
From raw data to mass estimation

- **Data processing:**
 - **Map-making**
 - Quantifying data processing filtering (transfer function)
- From maps to pressure profiles:
 - Point sources contamination
 - Pressure profile reconstruction
- Hydrostatic mass estimation

Map-making: CLJ1227 seen by NIKA2

Observed for 3.6h during the 15th NIKA2 run (N2R15, Feb. 13-20 2018, NIKA2 Guaranteed Time)

Maps obtained with the PIIC (*Pointing and Imaging In Continuum*) IRAM pipeline



5' maps, with a 10'' FWHM smooth

28.06.2021

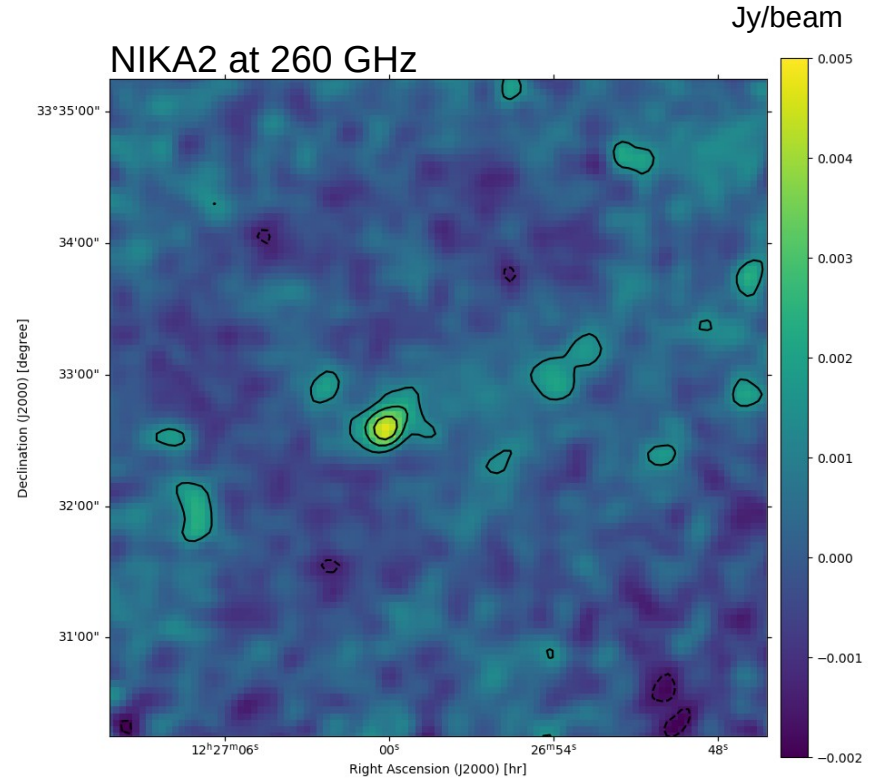
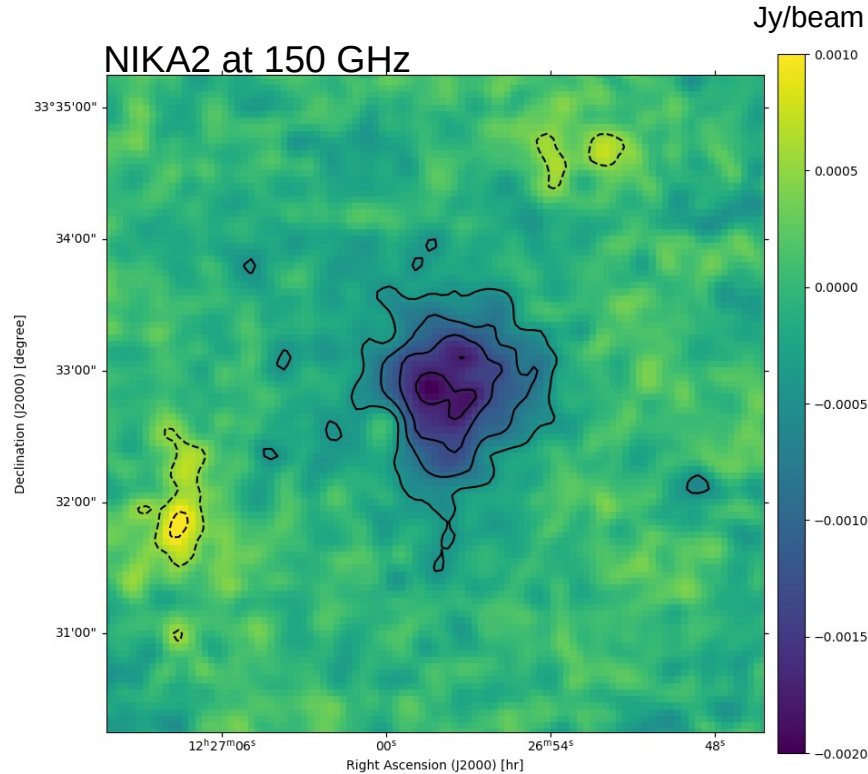
Miren Muñoz Echeverría

5 / 24

Map-making: CLJ1227 seen by NIKA2

Observed for 3.6h during the 15th NIKA2 run (N2R15, Feb. 13-20 2018, NIKA2 Guaranteed Time)

Maps obtained with the NIKA2 collaboration's IDL pipeline



5' maps, with a 10'' FWHM smooth. Contours are multiples of 3σ .

Maps used for the following analysis in this presentation

From raw data to mass estimation

- **Data processing:**
 - Map-making
 - **Quantifying data processing filtering (transfer function)**
- From maps to pressure profiles:
 - Point sources contamination
 - Pressure profile reconstruction
- Hydrostatic mass estimation

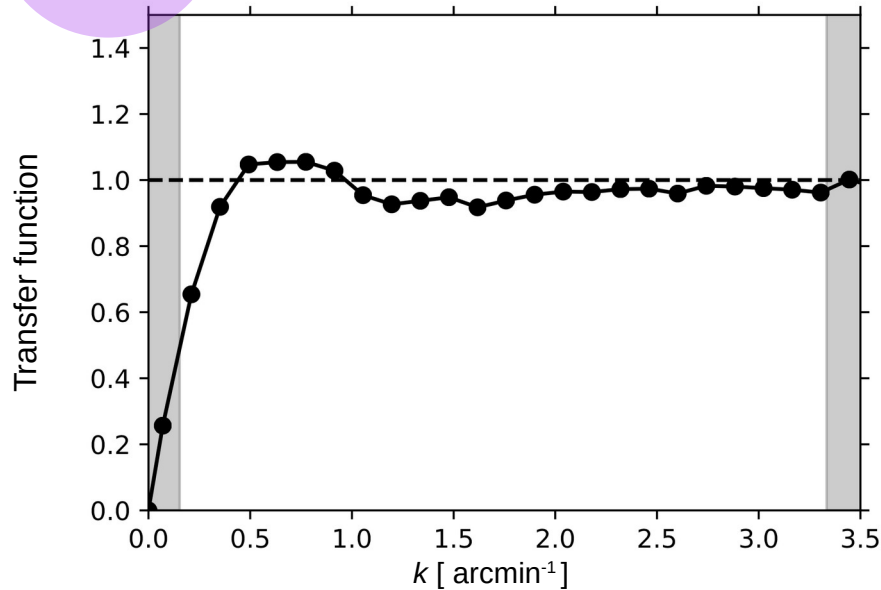
Quantifying data processing filtering: transfer function

Filtering estimated for 150 GHz maps in Fourier space, computed using simulations

$$\text{signal}_{\text{processed}} = \text{TF} * \text{signal}_{\text{in}}$$

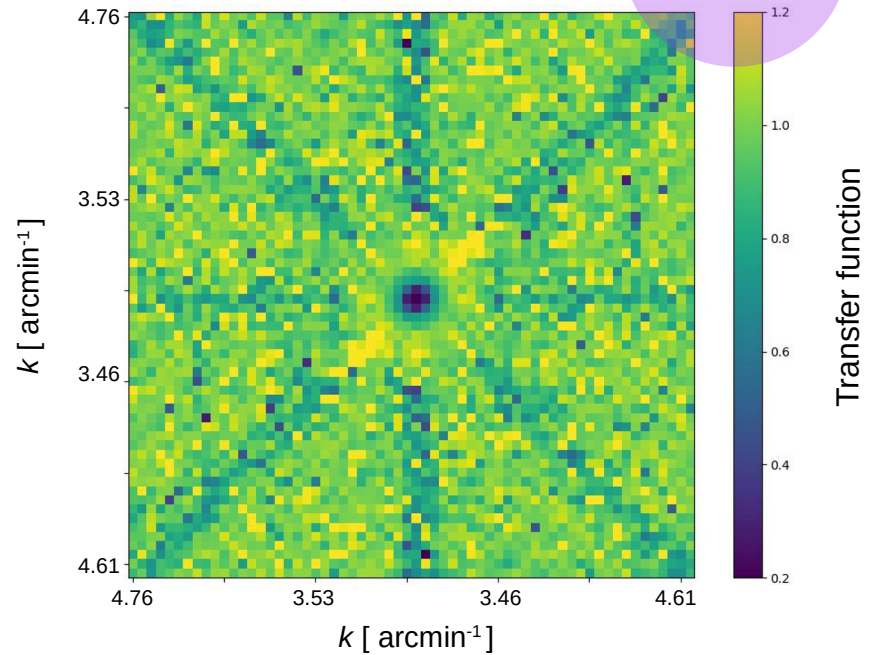
Standard LPSZ analysis

1D TF: circular symmetry



New approach

2D TF



2D transfer function allows us to deal with scanning angle effects

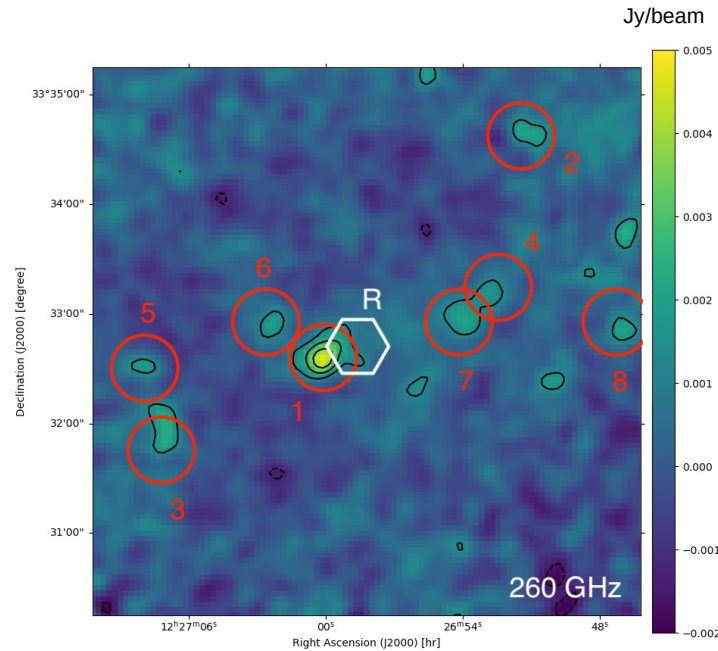
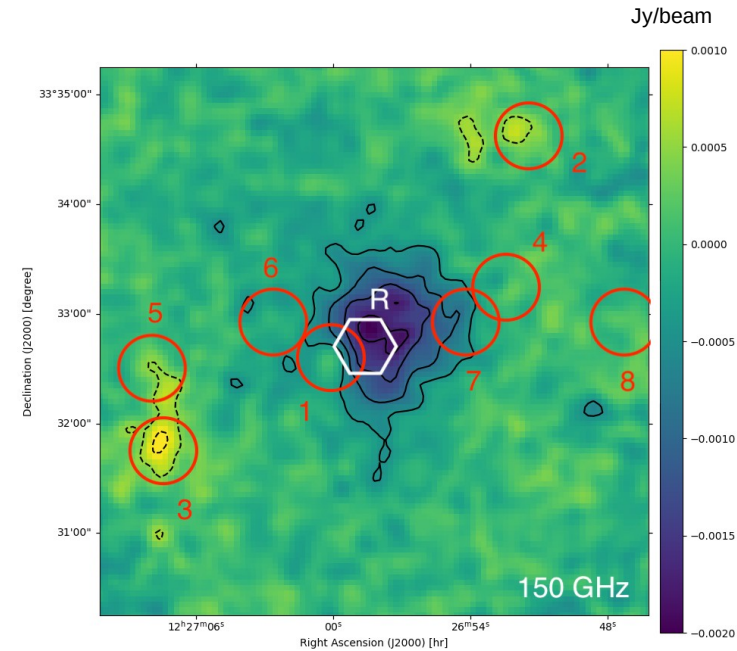
From raw data to mass estimation

- Data processing:
 - Map-making
 - Quantifying data processing filtering (transfer function)
- **From maps to pressure profiles:**
 - **Point sources contamination**
 - Pressure profile reconstruction
- Hydrostatic mass estimation

Point sources

Goal: to estimate their flux at 150 GHz

Identification



Submillimeter sources:

- NIKA2 maps (150 & 260 GHz)
- *Herschel* SPIRE (600, 860 & 1200 GHz) and PACS (1800 & 3000 GHz) catalogues

Radio source:

- VLA FIRST catalogue (1.4 GHz)

8 sub-mm and 1 radio sources identified

28.06.2021

Miren Muñoz Echeverría

10 / 24

Point sources

Goal: to estimate their flux at 150 GHz

Estimation of the flux at 150 GHz

Submillimeter sources:

Using PSTools by F. K eruzor e

1. Measurement of the flux in the 260 GHz NIKA2 map
2. Fit of a modified blackbody spectrum

$$F_\nu(F_0, \beta, T) = F_0 \left(\frac{\nu}{\nu_0} \right)^\beta B_\nu(T)$$

3. Extrapolation to 150 GHz

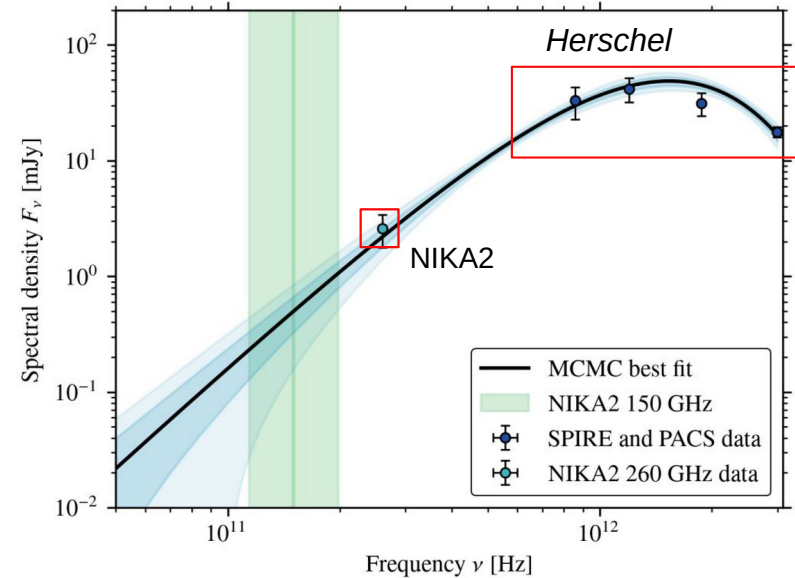
→ used as prior in the official LPSZ code `panco2`

Radio source:

1. Supposing a $F(\nu) = F(\nu_0) \times (\nu/\nu_0)^\alpha$ spectrum with $\alpha = -0.7 \pm 0.2$ and 3.60 ± 0.13 mJy at 1.4 GHz: at 150 GHz ~ 0.1 mJy

→ not considered

Spectral density distribution for PS4



From raw data to mass estimation

- Data processing:
 - Map-making
 - Quantifying data processing filtering (transfer function)
- **From maps to pressure profiles:**
 - Point sources contamination
 - **Pressure profile reconstruction**
- Hydrostatic mass estimation

Pressure profile determination

MCMC fit of electronic pressure profile and point sources to the NIKA2 150 GHz map using `panco2`

+ in F. Kéruzoré's talk

$$\text{MODEL}_{150\text{GHz}}^{(x,y)} = \underbrace{C_{150\text{GHz}}^{(x,y)}}_{\text{Calibration}} \left(\frac{\sigma_T}{m_e c^2} \int P_e dl \right)_{\text{cluster}} + \sum_{\text{Sources}} g_{2D}(F_{150\text{GHz}}, 17,7'') + \text{Zero}$$

- Calibration

- TF
- beam

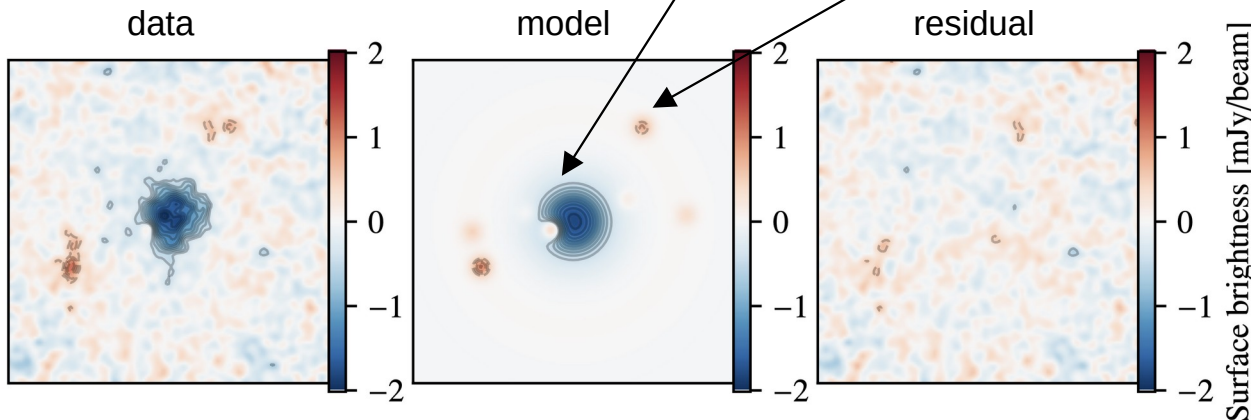
Two pressure models:

gNFW

$$P_e(r) = \frac{P_0}{\left(\frac{r}{r_p}\right)^c \left(1 + \left(\frac{r}{r_p}\right)^a\right)^{\frac{b-c}{a}}}$$

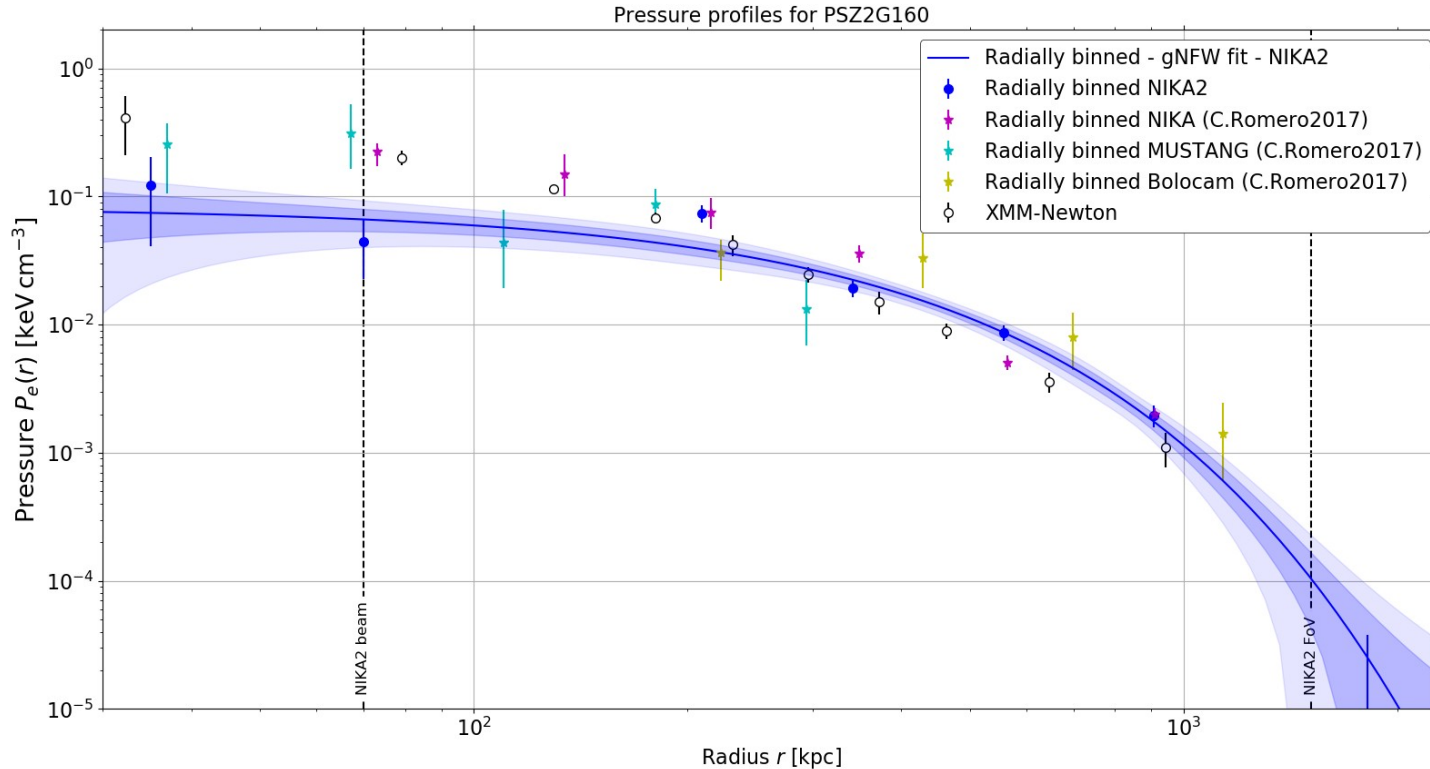
Radially binned model

$$P_e(r) = P_i \left(\frac{r}{r_i}\right)^{-\alpha_i}$$



Pressure profile for reference model

Radially binned model with 1D transfer function



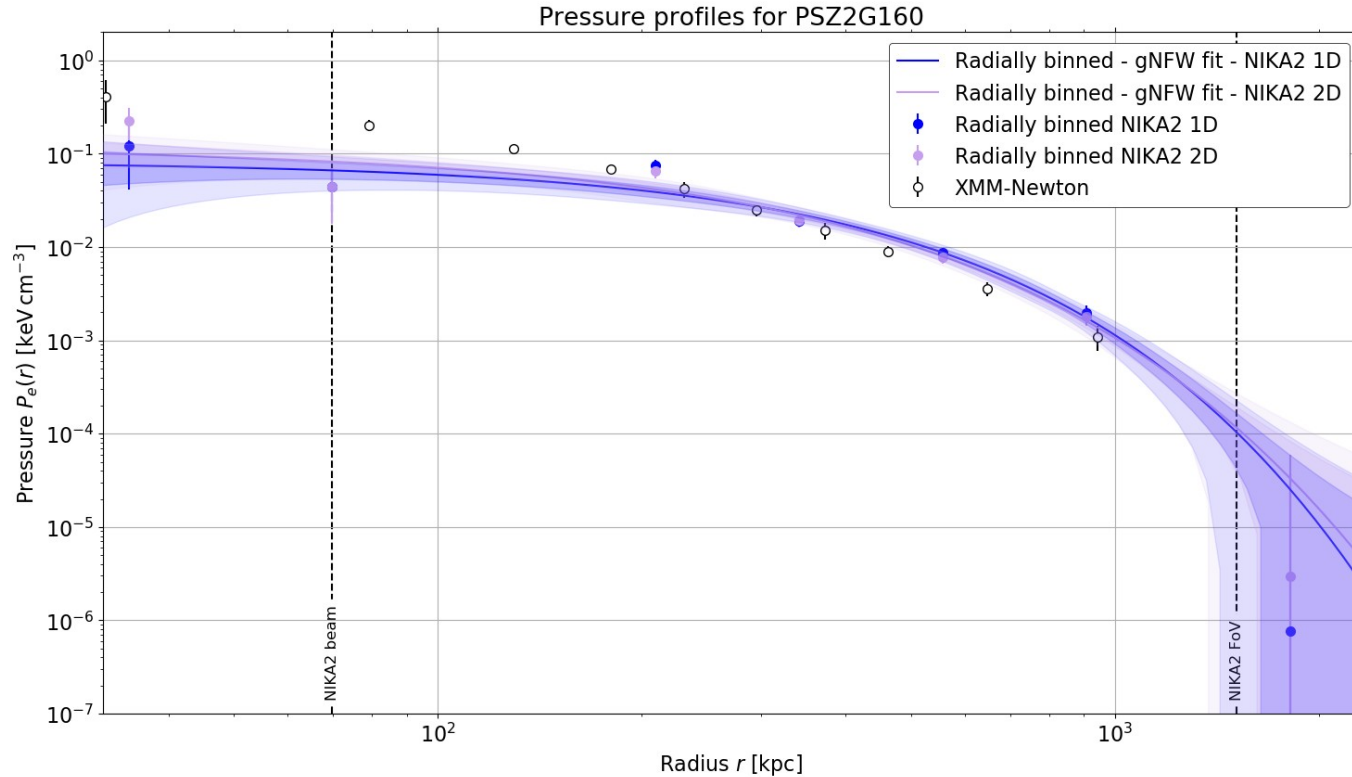
Consistent at large radii with other measurements. Discrepancy in the core with NIKA and XMM-Newton, but consistent with MUSTANG.

From raw data to mass estimation

- Data processing:
 - Map-making
 - Quantifying data processing filtering (transfer function)
- **From maps to pressure profiles:**
 - Point sources contamination
 - **Pressure profile reconstruction: ROBUSTNESS TESTS**
- Hydrostatic mass estimation

Pressure profile reconstruction: filtering effects

1D & 2D transfer function



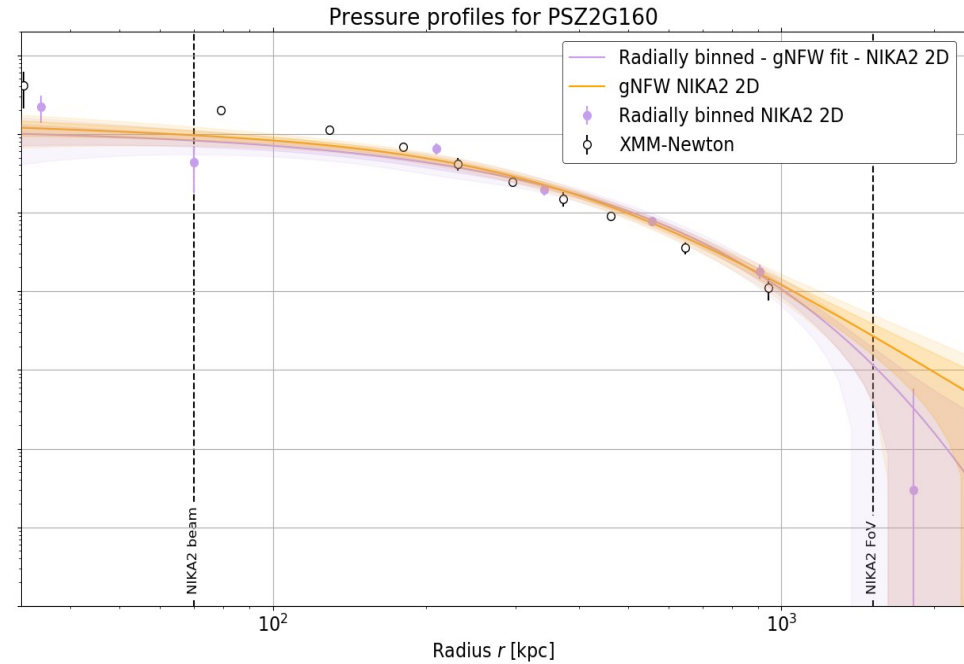
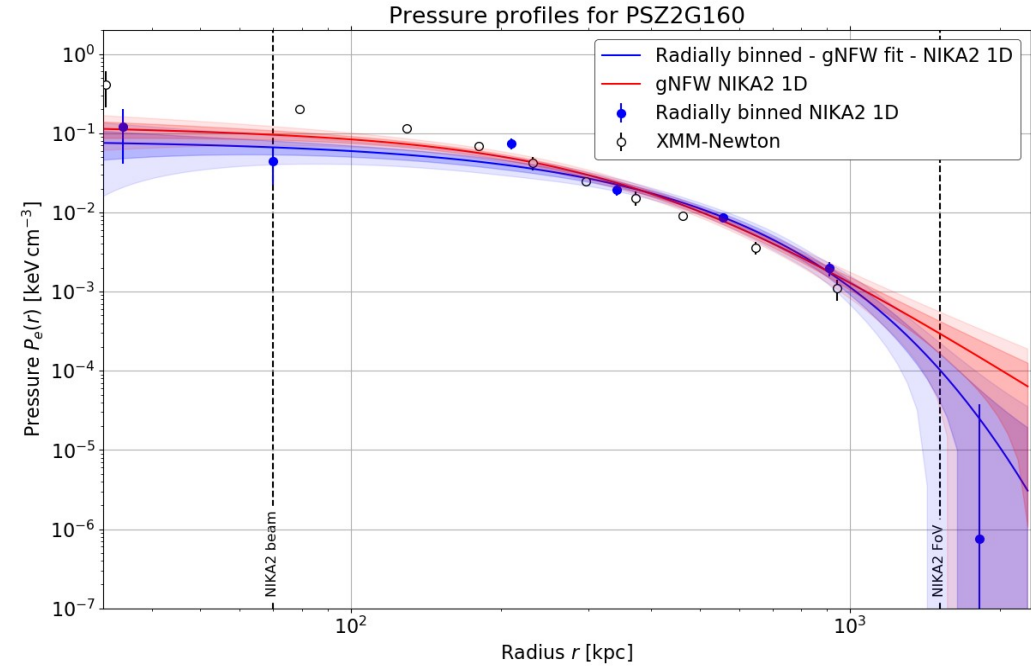
Scan direction filtering effects do not affect the reconstructed pressure profile

Pressure profile reconstruction: modelling effects

Rially binned & gNFW

1D TF

2D TF



Reconstructed pressure profiles are consistent within $1-\sigma$. No significant effects from modelling.

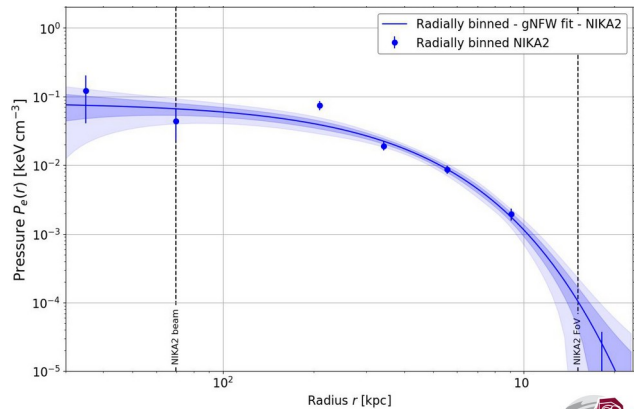
From raw data to mass estimation

- Data processing:
 - Map-making
 - Quantifying data processing filtering (transfer function)
- From maps to pressure profiles:
 - Point sources contamination
 - Pressure profile reconstruction
- **Hydrostatic mass estimation**

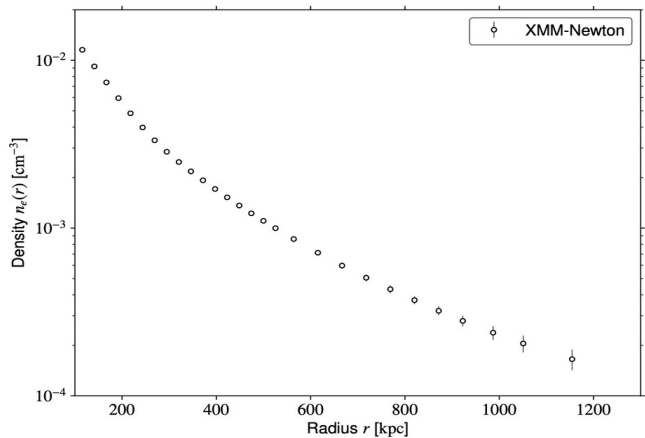
Hydrostatic mass profile

Applying the hydrostatic equilibrium hypothesis

With: P_e from SZ with **NIKA2**

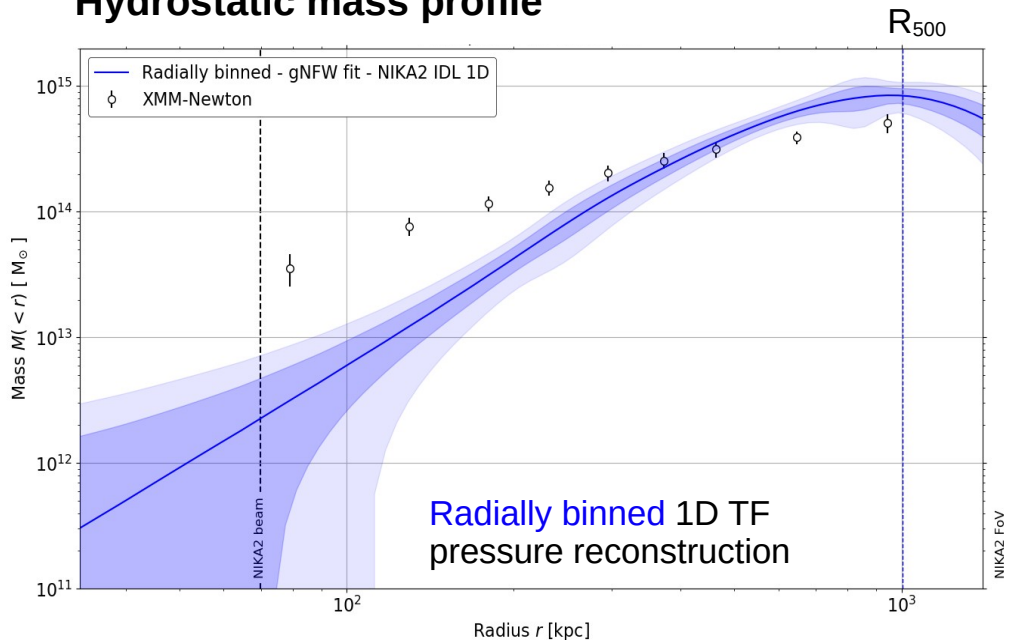


n_e from X with **XMM-Newton**



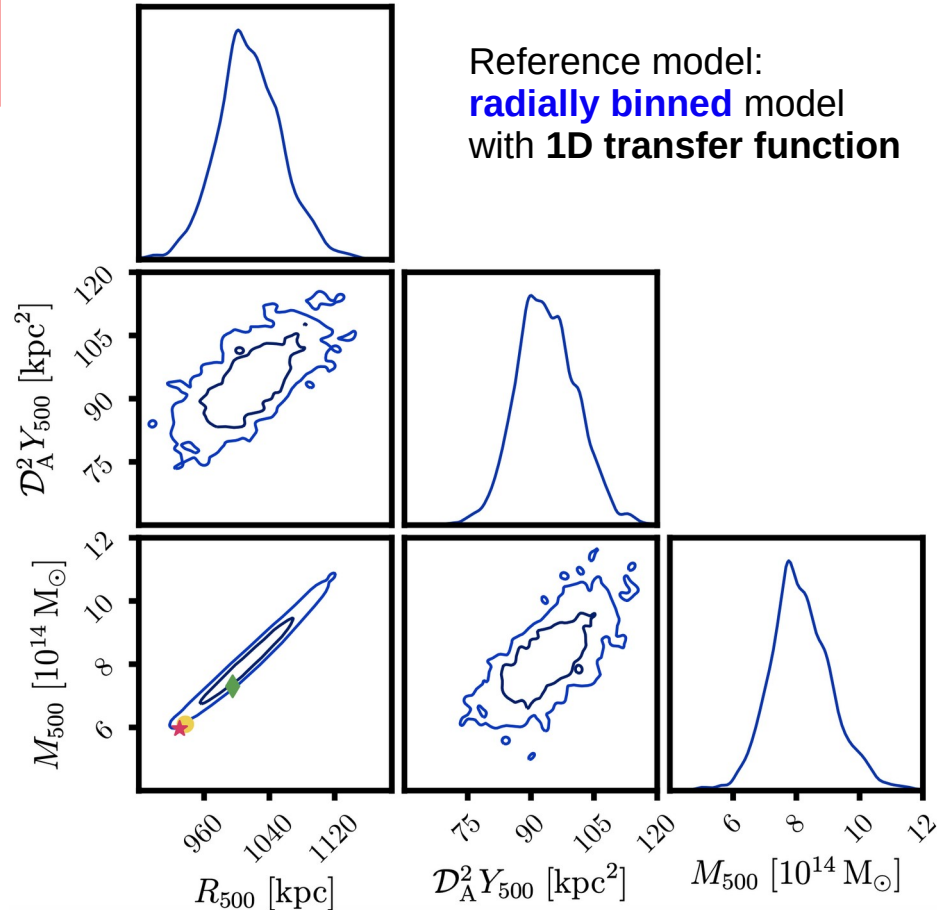
$$\frac{dP}{dr} = -\rho g = -\rho \frac{GM_{HSE}(r)}{r^2}$$

Hydrostatic mass profile



M_{500}^{HSE} is calculated in the extrapolated region
 Very sensitive to the estimate of the pressure slope

Integrated values: R_{500} - Y_{500} - M_{500}^{HSE}



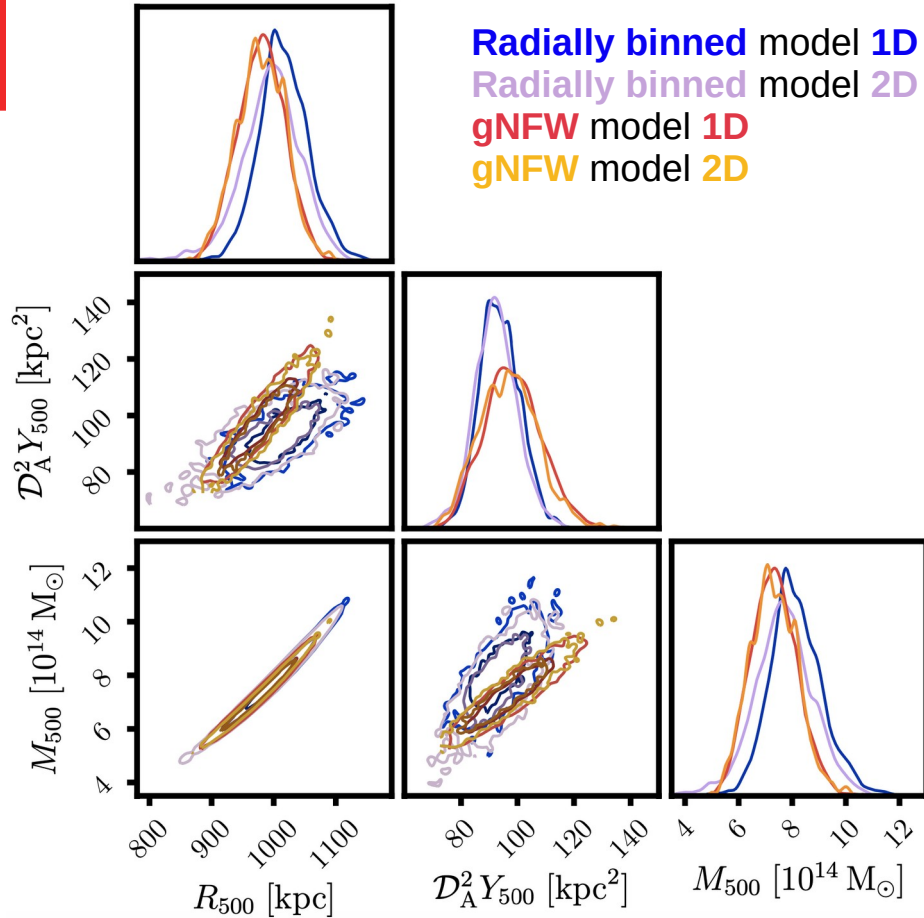
Other M_{500}^{HSE} estimations

Data	M_{500} [$10^{14} M_{\odot}$]	R_{500} [kpc]
★ NIKA PPC (R.Adam et al., 2015)	$5.96^{+1.02}_{-0.79}$	930^{+50}_{-43}
● NIKA FPC (R.Adam et al., 2015)	$6.10^{+1.52}_{-1.06}$	937^{+72}_{-58}
◆ NIKA NNN (R.Adam et al., 2015)	$7.30^{+1.52}_{-1.34}$	995^{+65}_{-65}
XMM-Newton (this data)	$5.95^{+0.23}_{-0.22}$	915^{+11}_{-11}
XMM-Newton + Chandra (Maughan et al., 2007)	$5.2^{+1.0}_{-0.8}$	880 ± 50

M_{500} and R_{500} are very correlated
 Only comparing the marginalized estimates may be misleading

→ we need to compare the posterior distributions

Robustness tests on integrated values: R_{500} - Y_{500} - M_{500}^{HSE}



Using 2D transfer function gives slightly lower R_{500} and M_{500} distributions for radially binned

The mass seems a bit tighter constrained using gNFW

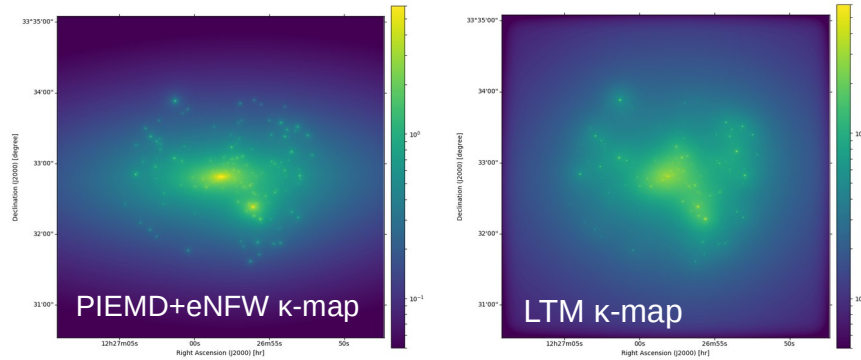
No big impact from pressure modelling if pressure derivative computed in a consistent way

Mass estimation seems robust against tested systematics, we measure $M_{500}^{\text{HSE}} = (7.65 \pm 1.03) \times 10^{14} M_\odot$

Similar results obtained with PIIC (IRAM's pipeline) maps

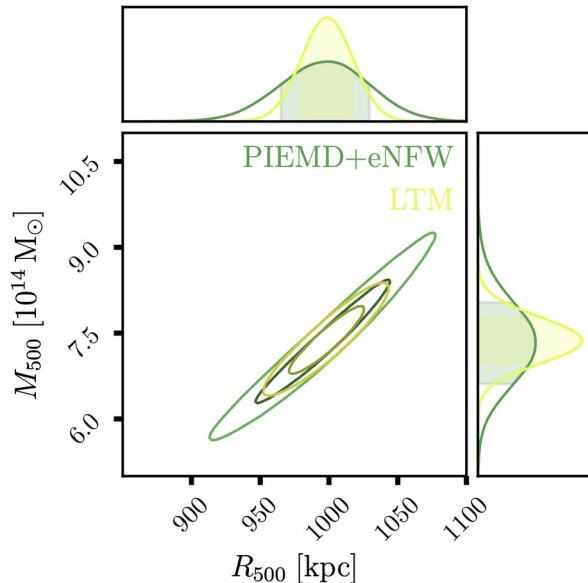
Lensing integrated values: $M_{500}^{\text{LENS}} - R_{500}$

Using **convergence maps** from **CLASH (Hubble)** and based on A. Ferragamo's work



+ in Wednesday's talk

(Zitrin et al., 2015)



We measure $M_{500}^{\text{LENS}} = (7.35 \pm 0.65) \times 10^{14} M_{\odot}$

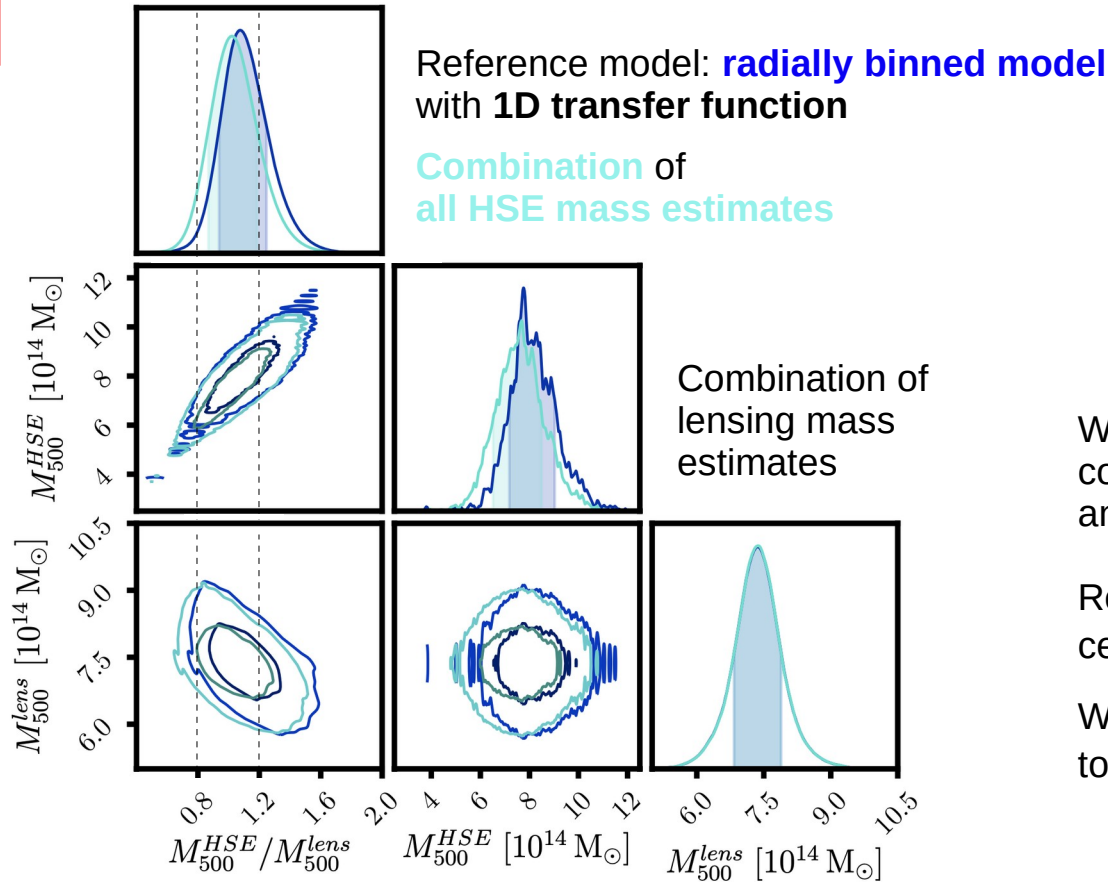
Robust lensing mass estimate, consistent with previous results
 ~ 10 % statistical uncertainties + less than 1 % systematics

Other M_{500}^{LENS} estimations

Data	$M_{500} [10^{14} M_{\odot}]$	$R_{500} [\text{kpc}]$
Hubble ST (M.Jee and J.Tyson, 2009)	$7.34 \pm 0.71^*$	*Calculated at the R_{500} by Maughan et al., 2007

Hydrostatic to lensing mass bias: $b_{\text{HSE/LENS}}$

$$M_{500}^{\text{HSE}}/M_{500}^{\text{LENS}} = (1 - b_{\text{HSE/LENS}})$$



We combine the posterior distributions for all the considered cases to account for data processing and modelling systematic effects

Reference model gives a bias w.r.t. lensing centered in $b_{\text{HSE/LENS}} < 0$; $M_{500}^{\text{HSE}} > M_{500}^{\text{LENS}}$

When accounting for systematics small change towards $b_{\text{HSE/LENS}} = 0$

Conclusions

- Combining **SZ and X-ray data** we have obtained **hydrostatic mass estimates for CLJ1227**, which is a **high redshift** cluster
For its the determination of **pressure profile derivatives is key**: in this work always deriving a gNFW
We have demonstrated that our hydrostatic mass estimates are robust against **filtering** and **pressure modelling**
- We find **no hydrostatic to lensing mass bias** for CLJ1227. We have measured $M_{500}^{\text{HSE}} = (7.65 \pm 1.03) \times 10^{14} M_{\odot}$ and $M_{500}^{\text{LENS}} = (7.35 \pm 0.65) \times 10^{14} M_{\odot}$
- This analysis allowed us to develop a standard pipeline to compare and combine hydrostatic and lensing mass estimates **+ see Wednesday's talk**
- To go beyond the current knowledge on CLJ1227: interferometer data from NOEMA to study the core and radio data to learn about non-thermal pressure